International Journal of Microwave and Wireless Technologies

cambridge.org/mrf

Investigation of a high-gain and broadband circularly polarized monopole antenna for RF energyharvesting application

Bikash Ranjan Behera and Sanjeev Kumar Mishra

Advanced RF and Microwave Lab, Department of Electronics and Communication Engineering, International Institute of Information Technology Bhubaneswar, Odisha 751003, India

Research paper

Cite this article: Behera BR, Mishra SK (2023). Investigation of a high-gain and broadband circularly polarized monopole antenna for RF energyharvesting application. *International Journal of Microwave and Wireless Technologies* **15**, 781–792. https://doi.org/10.1017/S1759078722000988

Received: 22 April 2022
Revised: 17 August 2022
Accepted: 18 August 2022

Key words:
Circular polarization (CP); improved radiation strength; high antenna gain; metasurfaces (MTS); printed monopole antenna; RF energy harvesting application

Author for correspondence:
Bikash Ranjan Behera,
E-mail: bikash.r.behera@ieee.org

Abstract

In this research article, a metasurface (MTS)-loaded high-gain and broadband circularly polarized (CP) monopole antenna is reported. The proposed antenna configuration consists of a symmetric Y-shaped radiating monopole over a partial ground plane with extended twin parasitic conducting strips (PCS) loaded with a MTS reflector. To achieve left-hand circular polarization characteristics, a metallic copper strip is utilized to short the partial ground plane with one of the twin PCS [PCS(L)]. By using the grid-slotted sub patches on a rectangular MTS a reflector of $2\lambda_{fa} \times 1.65\lambda_{fa} \times 0.02\lambda_{fa}$ is placed just below the monopole radiator at a height of $0.33\lambda_{fa}$, which provides broadened impedance (IBW) and 3 dB axial ratio bandwidth (ARBW) responses with high gain. The proposed prototype with an volumetric dimension of $1.33\lambda_{fa} \times 0.9\lambda_{fa} \times 0.02\lambda_{fa}$ at $f_a = 5$ GHz is designed and characterized. It exhibits a measured IBW of 48.45% (3.57–5.89 GHz), ARBW of 25.25% (4.21–5.42 GHz), and CP gain of > 8.35 dBic with the antenna efficiency of > 75% in the desired operating frequency bands. The obtained performances of the proposed MTS antenna confirm its suitability for RF energy harvesting application.

Introduction

With the development of RF applications in sub-6 GHz frequency bands, there is a significant requirement of antennas operating in the spectrum (i.e., operating bands) like LTE (3.5 GHz), Wi-Fi (5 GHz), WiMAX (3.5/5.5 GHz), ISM (5 GHz), 5G (5 GHz), and WLAN (IEEE 802.11 b/g/n/ac). Due to the availability of RF signals in the environment, RF front-ends are considered as the intrinsic part of communication system [1, 2]. Their effectiveness is assessed with the features of circular polarization (CP) [2–4]. Hence, in this present context, different kinds of antennas of numerous geometries have been investigated in [5–10]. But they exhibit narrow bandwidth(s), low gain, and poor efficiency. To overcome such type of limitations, CP antennas based on the metamaterials [11–14], slots [15–19], modification in the ground plane [20], incorporation of fractal phenomena [21], and change in the feeding mechanism [22, 23] have been reported. The implementation of metasurface (MTS) structures such as artificial magnetic conductors, electromagnetic bandgap structures, and reactive impedance surface are used as possible solution. Thus, the several types of multi-layered antennas have been explained in [24–34]. The antennas witness the limitations such as high profile, narrow impedance bandwidth (IBW) responses, and poor CP performances, as shown in Table 1. In this work, a MTS inspired circularly polarized symmetric Y-shaped printed monopole antenna (SYPMA-MTS) is designed to achieve better antenna performances and overcomes the challenge of complexity, over the existing ones. The key contributions of this proposed work are highlighted as follows:

(i) SYPMA is chosen as a radiator due to low-profile characteristics, less expensive, reasonable efficiency, stable radiation pattern, good time domain utility, and easy to analyze. Previously, antenna designs covering the Wi-Fi (5 GHz), Wi-MAX (3.5/5 GHz), ISM (5 GHz), and 5G (5 GHz) bands have been discussed in [35–37], but the non-existence of CP attributes fails to support their creditability from the applications point of view [38].
(ii) The CP radiation is achieved by shorting a metallic copper strip between partial ground plane and one of the twin parasitic conducting strips [PCS(L)]. Thus, a simple method is proposed to achieve the CP radiation from the LP monopole radiator.
(iii) In the present literature, none of the papers reported in [5–37] have highlighted the intuition for achieving CP traits [39, 40].
(iv) With incorporation of MTS reflector in a single-layer, there is a vital improvement of IBW and axial ratio bandwidth (ARBW) responses (i.e. broadband features) with

Table 1. Performance characteristics of the proposed metasurface antenna (SYPMA-MTS) over the existing ones reported in the literature [5–37, 39, 40]

Ref.	Antenna configuration	IBW	ARBW	CP gain $^{avg.}$
5.	Embedded patch antenna	Multi-bands	2.3%	4.4 dBic
6.	Stacked patch antenna	27.7%	11.47%	4.5 dBic
7.	Metamaterial antenna	Multi-bands	—	—
8.	PIFA reconfigurable antenna	Multi-bands	—	—
9.	Shorted patch antenna	3.25%	0.682%	3.8 dBic
10.	Conventional monopole antenna	152%	—	—
11.	CRLH-TL based antenna	0.62%	0.18%	6.97 dBic
12.	ENG-TL based antenna	5.8%	1.2%	8.28 dBic
13.	Metasurface-based metamaterial antenna	3.77%	1.86%	6.3 dBic
14.	Metamaterial antenna	3.9%	2.2%	1 dBic
15.	Slotted patch antenna	2%	0.7%	3.8 dBic
16.	Microstrip patch antenna + parasitics	6%	3.3%	2.7 dBic
17.	Slotted patch antenna	15.2%	3.2%	4.1 dBic
18.	Slotted dielectric resonator antenna	20.79%	12.03%	4.71 dBic
19.	Slotted dielectric resonator antenna	31%	18.2%	4.5 dBic
20.	Conventional monopole antenna	Multi-bands	5.1%	4.1 dBic
21.	Conventional dielectric resonator antenna	35.59%	11.57%	2.68 dBic
22.	Conventional dielectric resonator antenna	26.84%	17.59%	3.86 dBic
23.	Microstrip patch antenna	1.8%	0.6%	4.2 dBic
24.	Metasurface-based monopole antenna	16%	10%	5.5 dBic
25.	Metasurface-based slotted antenna	22.6%	14.3%	4.2 dBic
26.	Metasurface-based monopole antenna	33.7%	16.5%	5.8 dBic
27.	Metasurface-based monopole antenna	34.3%	18.69%	5.1 dBic
28.	Metasurface-based dipole antenna	16.8%	18%	4.8 dBic
29.	Metasurface-based slotted antenna	29.41%	9.05%	6.34 dBic
30.	Metasurface-based Eng-TL CSRR antenna	16.36%	11.93%	5.62 dBic
31.	Metasurface-based reconfigurable antenna	31.6%	20.8%	6.9 dBic
32.	Metasurface-based reconfigurable antenna	20.5%	15.5%	4.25 dBic
33.	Metasurface-based reconfigurable antenna	25%	25%	6.6 dBic
34.	Metasurface-based microstrip patch antenna	20.6%	17.4%	8 dBic
35.	Conventional monopole antenna	154%	—	—
36.	Conventional monopole antenna	167%	—	—
37.	Conventional monopole antenna	Multi-bands	—	—
39.	Superstrate-based monopole antenna	114.9%	20.02%	6.82 dBic
40.	Metasurface-based monopole antenna	57.21%	25.25%	4.92 dBic
P1.	Y-shaped monopole antenna (SYPMA)	38.61%	6.82%	2.36 dBic
P2.	SYPMA loaded with single-layered metasurface (MTS) Reflector	48.45%	25.25%	8.45 dBic

Ref., reference; IBW, – 10 dB impedance bandwidth; ARBW, 3 dB axial bandwidth; —, not reported.

enhanced CP antenna gain of > 8.35 dBic, which offers better performance over the reported ones.

(v) In the next part of analysis, new theoretical insights taking into the account of 3 dB ARBW (BW3dB) and CP antenna gain (G_{3dB}) are presented to analyze the CP characteristics of any type of CP antennas using the equations (2)–(5).

(vi) The proposed antenna (SYPMA-MTS) can be used for RF energy harvesting (RF-EH) application. To test its capability for such a instance, it is integrated with the CRLH-based rectifier circuit, and the LC-based rectifier circuit, which is used to evaluate the RF-to-DC conversion efficiency (η_0) and DC output voltage (V_{out}) at 5 GHz bands using ADS circuit solver.

https://doi.org/10.1017/S1759078722000988 Published online by Cambridge University Press

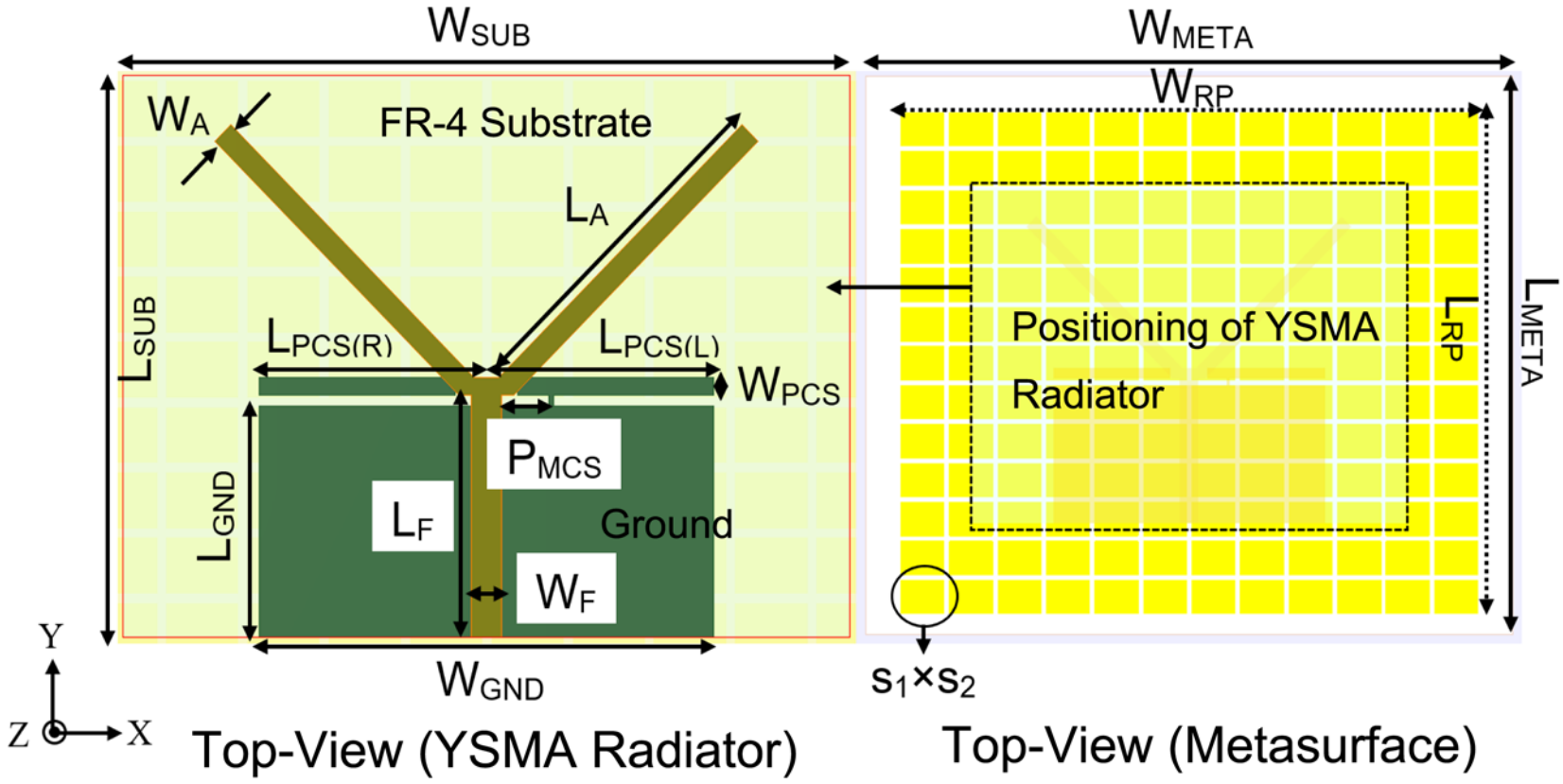

Fig. 1. Schematic configuration of the proposed broadband circularly polarized monopole antenna loaded with metasurface reflector. [The dimensions are as: $W_{SUB} = 1.33\lambda_0$, $L_{SUB} = 0.9\lambda_0$, $W_{GND} = 0.83\lambda_0$, $L_{GND} = 0.4\lambda_0$, $L_{PCS(R)} = 0.36\lambda_0$, $L_{PCS(L)} = 0.36\lambda_0$, $W_{PCS} = 0.03\lambda_0$, $P_{MCS} = 0.05\lambda_0$, $W_A = 0.04\lambda_0$, $L_A = 0.6\lambda_0$, $L_F = 0.42\lambda_0$, $W_F = 0.05\lambda_0$, $W_{RP} = 1.78\lambda_0$, $L_{RP} = 1.48\lambda_0$, and $S_1 \times S_2 = 0.13\lambda_0 \times 0.09\lambda_0$, where $\lambda_0 = 60$ mm.].

Table 1 presents the comparative study of SYPMA-MTS over the existing literatures in [5–37, 39, 40]. The utilization of MTS is also applicable to the other CP antennas for performance improvement in terms of broad 3 dB ARBW and CP antenna gain with the improved front-to-back ratio (FBR). Their design analogy, and its working mechanism, with corresponding outcomes, and their interpretation from application perspective are discussed in the subsequent sections.

Antenna design

Proposed antenna configuration

Figure 1 shows schematics of proposed antenna, printed on a FR-4 substrate ($\epsilon_r = 4.4$, $\tan\delta = 0.018$, $h_{sub} = 0.02\lambda_{fa}$) with the overall volumetric dimension of $1.33\lambda_{fa} \times 0.9\lambda_{fa} \times 0.02\lambda_{fa}$ (i.e. λ_{fa} is the free-space guided wavelength at 5 GHz). Here, authors have shorted the partial ground plane with one of the twin PCS [PCS(L)] of

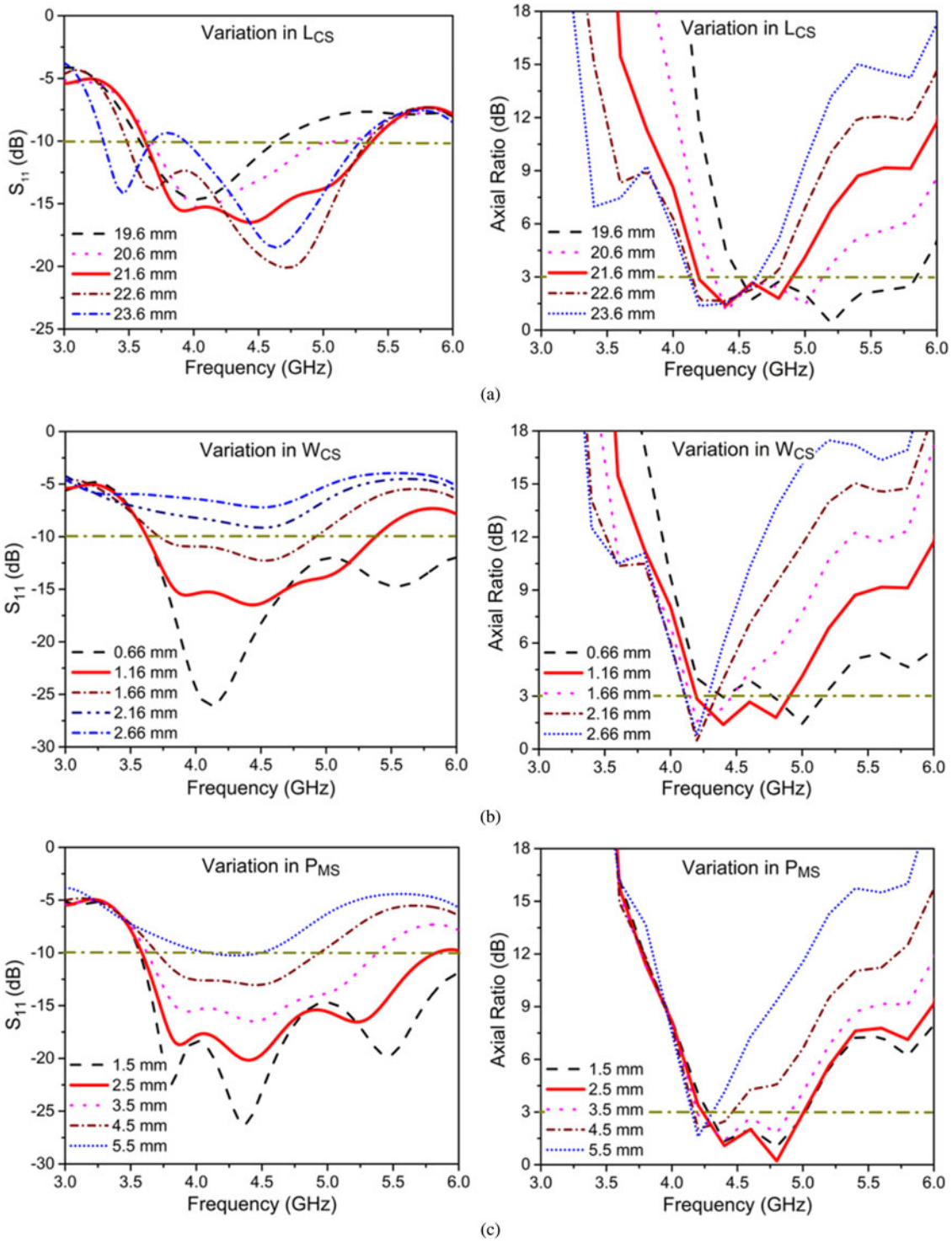

Fig. 2. Effects on the antenna metrics due to variation in (a) L_{CS}, (b) W_{CS}, and (c) P_{MS}.

https://doi.org/10.1017/S1759078722000988 Published online by Cambridge University Press

$0.36\lambda_{fa} \times 0.03\lambda_{fa}$. It is separated by $0.019\lambda_{fa}$ from the upper edges of conventional partial ground plane by using a metallic copper strip, which is responsible for achieving CP radiation attributes. Then, the rectangular-MTS reflector with a dimension of $2\lambda_{fa} \times 1.65\lambda_{fa} \times 0.02\lambda_{fa}$ is placed below the Y-shaped radiating monopole at a height of $0.33\lambda_{fa}$, which is supported by the four plastic spacers.

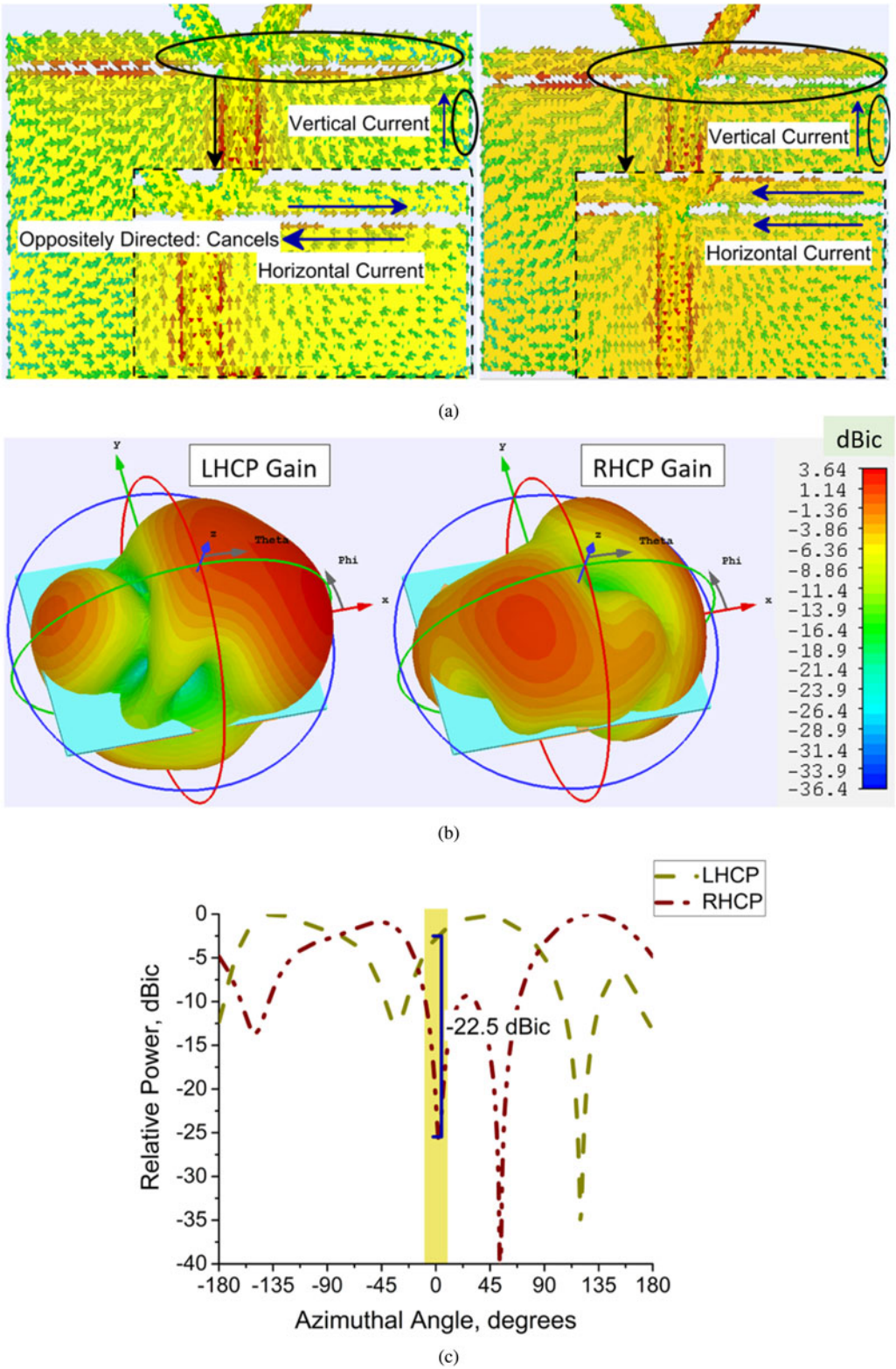

Fig. 3. Evaluation of CP mechanism at 5 GHz (a) surface current distribution [approach-I], (b) maximum realized gain [approach-II], and (c) relative power [approach-II] from normalized radiation pattern in the broadside direction for SYPMA.

https://doi.org/10.1017/S1759078722000988 Published online by Cambridge University Press

Parametric study

In this section, the design and its parametric analysis of proposed CP monopole antenna without MTS reflector is performed using CST microwave suite. Initially, the ground plane is optimized. It is observed that, if a large ground plane is used, then the S_{11} and AR will degrade, and there is a change of radiation pattern characteristics. The 3 dB axial ratio (AR) shows greater sensitivity to the width of the ground plane (W_{GND}), because of their dependency on horizontal components (horizontal currents). It is also sensitive to (a) length of the PCS (L_{CS}), (b) width of the PCS (W_{CS}), and (c) position of the metallic copper strip (P_{MS}). Thus, the current investigation dispenses that the variation of these geometrical parameters often puts significant impact on S_{11} and AR properties. The variations due to the L_{CS} on S_{11} and AR are highlighted in Fig. 2(a). At $L_{CS} = 21.6$ mm, the proposed antenna exhibits wider IBW and ARBW. A similar analogy is highlighted in Fig. 2(b), when $W_{CS} = 1.16$ mm is considered. With the due incorporation of twin PCS, impedance matching trait is improved. Furthermore, the positioning of metallic copper strip (P_{MS}) correlates with the phenomenon of shorting in between partial ground plane and PCS(L), which demonstrate the CP characteristics. In Fig. 2(c), the variation in P_{MS} and its impact on S_{11} and AR are highlighted. When $P_{MS} = 2.5$ mm, an optimum CP performance is observed in the desired operating bands.

Since, the design intuition is to achieve effectiveness in its performance, mutual inductance effects of the geometry that stabilizes to an extent, and optimizes the antenna performance to the final optimum with the objective to render out a simple, compact, and low-profile characteristics without affecting the fundamental characteristics from its physical insights.

Analysis of CP characteristics

In this case, the understanding of CP mechanism is interpreted by utilizing surface current distribution phenomenon [approach-I] and far-field radiation pattern [approach-II]. In approach-I, the understanding toward the existence of CP waves is often confirmed by the simultaneous presence of both horizontal and vertical currents on the antenna surface. Subsequently, for approach-II, the orientation of CP is observed by considering far-field analogy in broadside direction (ϕ=0^0 and $\theta = 0^0$), through maximum CP antenna gain [approach-II(a)] and relative power [approach-II (b)] obtained from the normalized radiation pattern. The analysis of CP mechanism is persuaded at $f_a = 5$ GHz, and the outcomes of both approaches are highlighted in Fig. 3. For approach-II(a), it is observed that left-hand CP (LHCP) gain is 2.32 dBic and right-hand CP (RHCP) gain of 2.2 dBic, which indicates that the proposed monopole antenna is of LHCP type. Similarly, in approach-II(b), it is observed that, LHCP is quite stronger than RHCP by -22.5 dBic. These combined results do confirm the nature of antenna as LHCP orientation. From the above analysis, it is inferred that approach-I correlates with the existence of CP characteristics, whereas the approach-II gives idea about the nature of CP for the proposed antenna.

Implementation of metasurface reflector

The execution of MTS reflector at a height of $0.33\lambda_{fa}$ below the SYPMA is implemented to achieve high CP antenna gain with directional characteristics. The proposed MTS with surface area of $1.78\lambda_{fa} \times 1.48\lambda_{fa}$ is used as a reflector. It consists of grid-slotted sub-patches of 12×12 cells, where each cell of $0.1\lambda_{fa} \times 0.06\lambda_{fa}$ is placed with an intermediate gap of $0.016\lambda_{fa}$ on the rectangular-shaped PEC body with the overall dimension of $2\lambda_{fa} \times 1.65\lambda_{fa} \times 0.02\lambda_{fa}$, combined together to form the rectangular-shaped MTS reflector. When this particular MTS layer comes in contact with SYPMA, it redirects one-halves of the radiated waves in the opposite direction. These radiated waves from SYPMA-MTS consist of the waves directed from SYPMA and waves reflected from the MTS reflector, transform the boresight radiation at both of radiated planes toward directional radiation pattern, with a FBR of –21.5 dBic and cross-polarization level of ≥ -22.5 dBic at the desired 5 GHz frequency bands.

In addition to above performances, average CP antenna gain is significantly improved to 3.59 times, i.e., 2.35–8.45 dBic but importantly, the IBW is improved to a fractional bandwidth of 48.45%, i.e., 1.08 times from 2.11 to 2.28 GHz and ARBW is also improved toward fractional bandwidth of 25.25%, i.e., 4.03 times from 300 MHz to 1.21 GHz. The insights behind achieving out such type of improvements lies with the intuition that by loading a MTS reflector layer, the dominant inductive coupling process takes place and that resulted in broadening bandwidth performances, i.e., IBW and 3 dB ARBW characteristics. Prior to this, whenever grid-slotted patches are introduced as the MTS layer, then there is the generation of higher-order modes [39], which is significantly responsible for the improved antenna bandwidth and its radiation strength.

A theoretical approach on analyzing CP characteristics

In the reported work, the theoretical insights [39] of 3 dB ARBW (BW_{3dB}) and CP antenna gain (G_{3dB}) are presented for the complete evaluation of antenna characteristics, especially for analyzing the CP characteristics of any type of CP antennas, irrespective of the geometry and frequency of operation. To understand such phenomena, let us consider the criteria (C_r) in a general form, expressed as:

$$C_r = \frac{BW_{3dB} \times G_{3dB}}{100} \tag{1}$$

Equation (1) is the basic form of the proposed criteria for analyzing CP attributes. It considers 3 dB axial bandwidth and CP

Table 2. Examination of metasurface-inspired CP antennas [24–34] w.r.t. the proposed antenna (SYPMA-MTS) for the criteria: C_{r1}, C_{r4}

Ref.	BW_{3dB}	$G_{3dB(avg)}$	$G_{3dB(peak)}$	C_{r1}	C_{r4}
24.	10%	5.5 dBic	6.67 dBic	0.55	0.67
25.	14.3%	4.2 dBic	4.8 dBic	0.61	0.68
26.	16.5%	5.8 dBic	5.8 dBic	0.95	0.95
27.	18.69%	5.1 dBic	6.1 dBic	0.95	1.14
28.	18%	4.8 dBic	6.8 dBic	0.86	1.22
29.	9.05%	6.34 dBic	6.34 dBic	0.57	0.57
30.	11.93%	5.62 dBic	5.94 dBic	0.67	0.71
31.	20.8%	6.9 dBic	6.9 dBic	1.43	1.43
32.	15.5%	4.25 dBic	4.25 dBic	0.65	0.65
33.	25%	6.6 dBic	6.6 dBic	1.65	1.65
34.	17.4%	8 dBic	8.3 dBic	1.39	1.44
P2.	25.25%	8.45 dBic	8.78 dBic	2.13	2.21

https://doi.org/10.1017/S1759078722000988 Published online by Cambridge University Press

antenna gain as the important parameters for RF front-end in RF-EH [39]. With the segregation of CP antenna gain and its evaluation in terms of (a) average (G_{avg}), (b) maximum (G_{max}), (c) minimum (G_{min}), and (d) peak (G_{peak}), the proposed criteria (C_r) can be further derived as C_{r1} to C_{r4}, shown in equations (2) to (5):

$$C_{r1} = \frac{BW_{3\text{dB}} \times G_{3\text{dB(avg)}}}{100} \quad (2)$$

$$C_{r2} = \frac{BW_{3\text{dB}} \times G_{3\text{dB(max)}}}{100} \quad (3)$$

$$C_{r3} = \frac{BW_{3\text{dB}} \times G_{3\text{dB(min)}}}{100} \quad (4)$$

$$C_{r4} = \frac{BW_{3\text{dB}} \times G_{3\text{dB(peak)}}}{100} \quad (5)$$

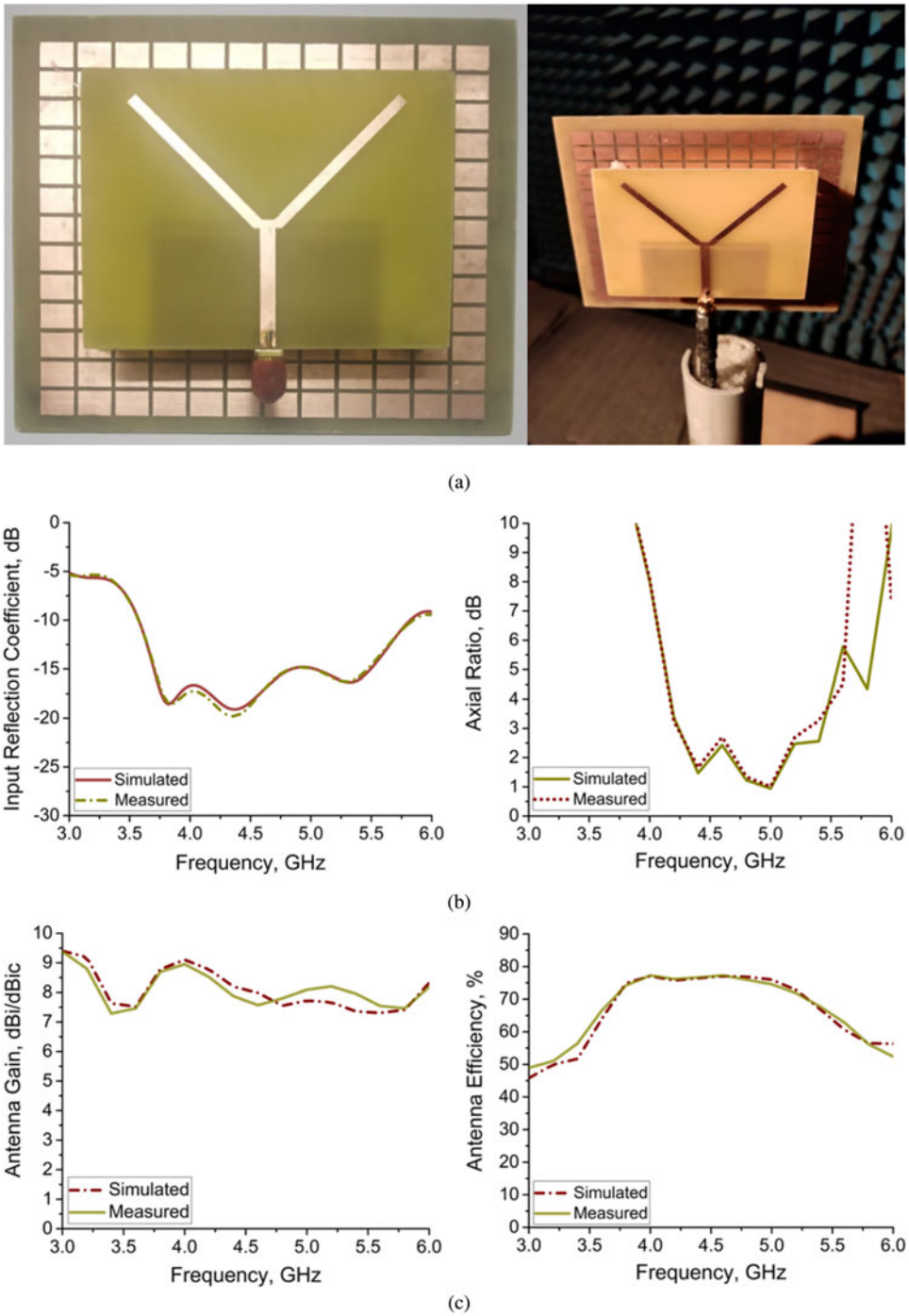

Fig. 4. Characterization of proposed antenna in terms of (a) antenna prototype and far-field pattern setup in anechoic chamber, (b) S_{11} and axial ratio (AR), and (c) antenna gain and efficiency.

https://doi.org/10.1017/S1759078722000988 Published online by Cambridge University Press

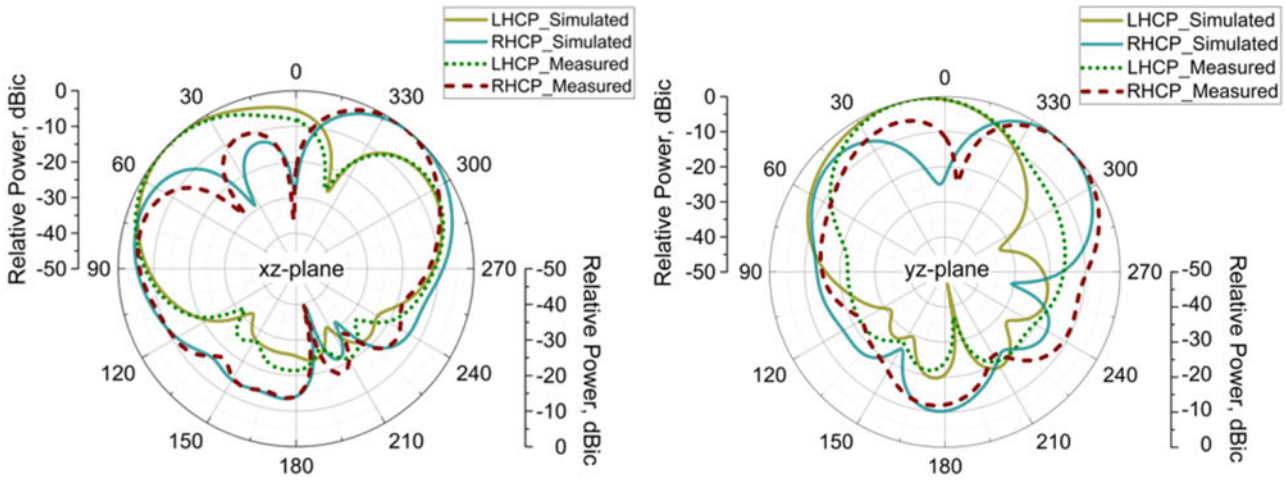

(a)

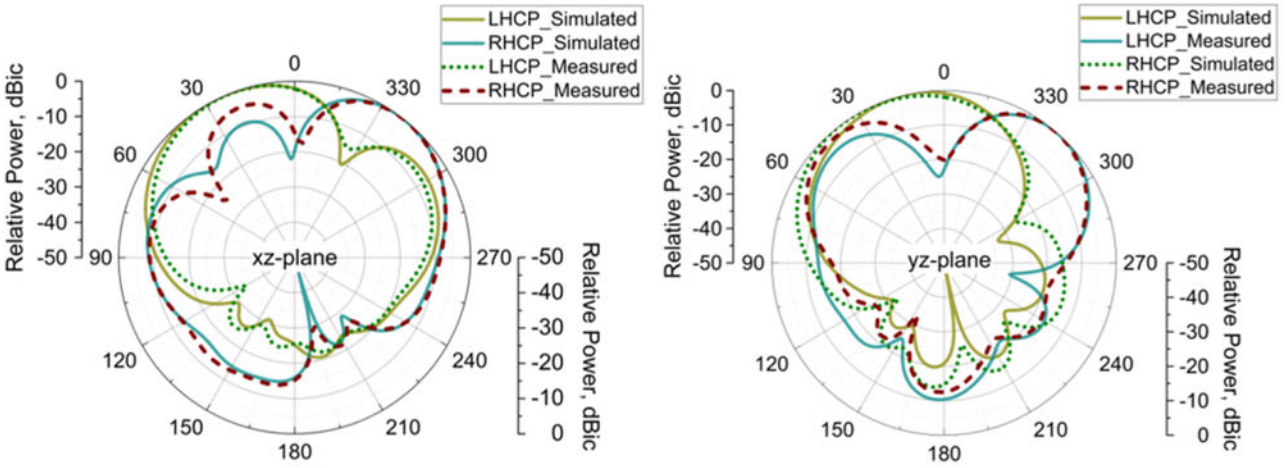

(b)

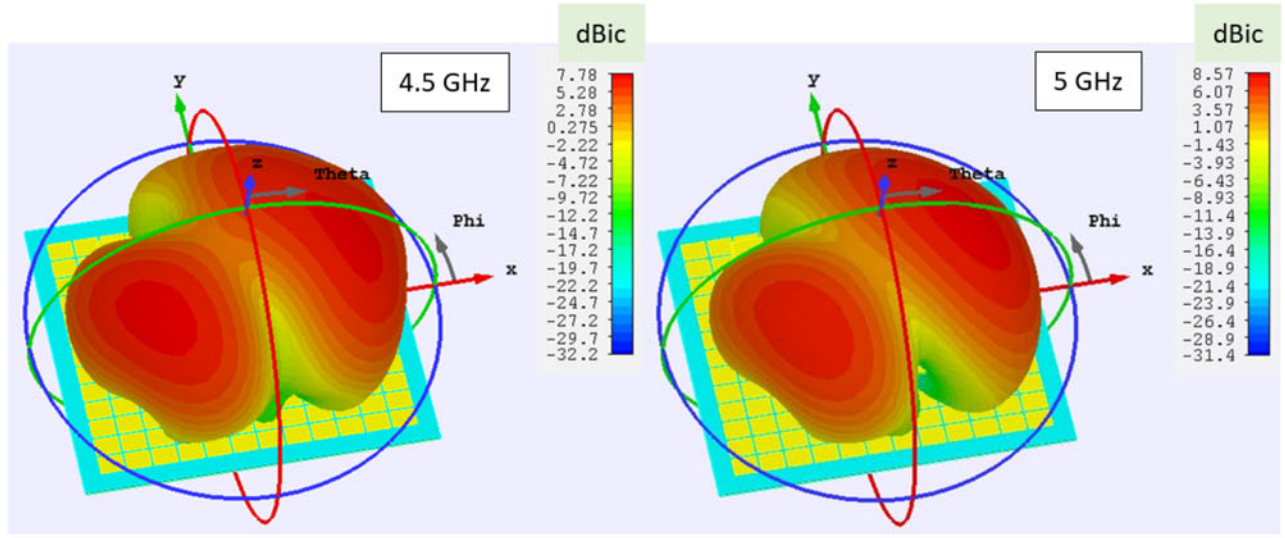

(c)

Fig. 5. Far-field radiation traits of SYPMA-MTS at (a) 4.5 GHz, (b) 5 GHz, with (c) 3D pattern at 4.5 and 5 GHz respectively.

https://doi.org/10.1017/S1759078722000988 Published online by Cambridge University Press

So, equations (2) to (5) are proposed for evaluating CP antenna characteristics. Their corresponding outcomes are shown in Table 2. Henceforth, an effective methodology is implemented for analyzing the RF front-ends based upon the bandwidth (ARBW) and CP gain characteristics.

Experimental results

To validate the performance of a proposed MTS loaded monopole antenna, prototype is shown in Fig. 4(a) fabricated by using ETS-PCBMATE prototyping machine. The S_{11} (dB) ismeasured by using PNA X-series Microwave Network Analyzer (N5247A) from

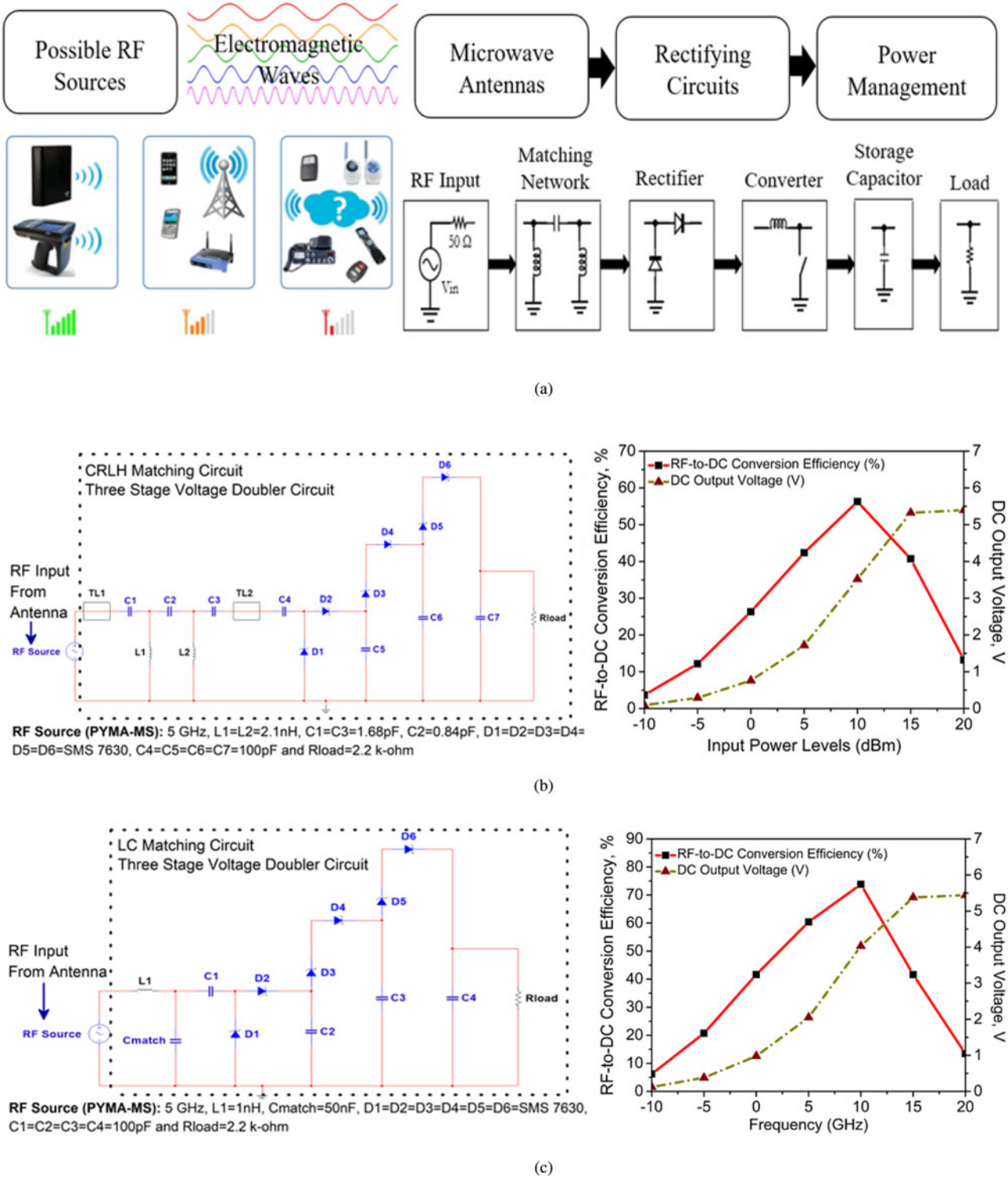

Fig. 6. Application perspective. (a) Block diagram of RF energy harvesting mechanism, (b) CRLH-based GVD circuit (I), and (c) LC-based GVD circuit (II).

https://doi.org/10.1017/S1759078722000988 Published online by Cambridge University Press

the Keysight Technologies, whereas the AR (dB), antenna gain, radiation pattern, and antenna efficiency are measured in the anechoic chamber. Figure 4(b) presents the S_{11} and AR plots. It exhibits ameasured IBW and ARBW of 48.45% (3.57–5.84 GHz) and 25.25% (4.21–5.42 GHz), which matches with that of the simulated outcomes.

The average simulated and measured antenna gain are > 8.35 dBic and antenna efficiency > 75% over the operating frequency bands, as presented in Fig. 4(c). The proposed antenna has a peak gain variation from 7.5 to 8.5 dBi. It is also observed that, MTS layer has a better performance compared to earlier reported antennas in [5–37, 39, 40], and witness better reflection properties due to the presence of coupling effects [41] of inductance and capacitance, which control the fringing fields to be effectively coupled out with the radiated fields. Here, the radiation pattern at different frequencies is measured in the anechoic chamber and their plots are presented in Figs 5(a) and (b). For the proposed MTS inspired antenna, centered at $f_a = 4.5$ and 5 GHz, radiation plots for the principal planes at $\phi = 0^{\circ}$ and $\phi = 90^{\circ}$ are highlighted with the directional pattern. Owing to the MTS reflector, it possesses stable FBR ranging from -15 to -21.5 dBic. Thus, the boresight radiation has a maximum intensity along $+z$-axis shown in Fig. 5(c). Hence, SYPMA-MTS has not only achieved performance trade-offs required from application perspective but also the proposed antenna design concept is a generic solution for achieving high CP performances.

Key design aspects of proposed antenna

- The size of printed monopole antenna (SYPMA) is less than the size of MTS reflector. Due to reduction in its size, the effective height is fixed at a gap of $0.33\lambda_{fa}$, for better impedance matching and stable boresight radiations.
- The radiator geometry in general reduces electrical footprint of antenna size. It is difficult to excite antenna with MTS reflector, that is why tuning of feeding mechanism and shorting process have been transformed, which transduces excitation of energy in an effective manner with the generation of CP characteristics.
- Here, the MTS reflector initiates the effective coupling process [41]. Due to the presence of such type of ground configuration, it emulsifies coupled energy into boresight radiation, so, there is no spurious nulls. It assists for radiation strength, as IBW, ARBW, and gain are enhanced with improved FBR. To demonstrate the low-profile and effectiveness, gap between the structures is fixed at $0.33\lambda_{fa}$, for the significant improvement of CP antenna gain.
- The proposed antenna satisfies impedance performances, antenna gain, radiation efficiency metrics from the application perspective.

Investigation toward RF energy harvesting

The proposed MTS antenna (SYPMA-MTS) is integrated with the CRLH and LC-based Greinacher voltage doubler circuits (GVDs), where RF-to-DC conversion efficiency (η_0, %) and DC output voltage (V_{out}, V) are calculated by using the ADS solver. The complete block diagram of RF-EH mechanism, and its corresponding outcomes for the two different designed rectifier circuits are shown in the Figs 6(a)–(c). In general, the selection of rectifier topology [42–47] is important in RF energy harvester design. Among the available and reported topologies of rectifier in literature, voltage doublers are considered as best choice for RF-to-DC rectification, due to simplicity of design and better power handling capability. In the another aspect, diode is considered as the main rectifying element in a GVD, and it influences the overall performance of the circuit. The parameters which play an important part in the selection of the diode/s are series resistance (R_s), junction capacitance (J_c), threshold voltage (V_t), and the breakdown voltage (V_b). To select the best diodes operating at 5 GHz frequency bands, some commercially available RF-diodes are listed along with their properties in Table 3.

Table 3. Commercially available Schottky diodes for rectification

Diode series	R_s	J_c	V_t	V_b
HSMS-2860	6 Ω	0.18 V	0.65 V	7 V
HSMS-8202	14 Ω	0.26 V	0.35 V	4 V
SMS-7630	20 Ω	0.14 V	0.34 V	2 V
SMS-7621	12 Ω	0.1 V	0.55 V	3 V
MA-40417	4.9 Ω	0.04 V	0.65 V	11 V

In Table 3, SMS-7630 has the minimum value for V_t, which implies that, it will turn ON for the minimum input power, and is considered as a best choice for harvesting DC power from the low-level ambient RF signals. In such a scenario, the impedance matching network is of huge significance for maintaining the overall efficiency (η_0) of the circuit. In this concurrent analysis, CRLH-TL and LC-based matching GVD circuits are proposed and investigated for the 5 GHz bands.

In general, CRLH type of matching circuit is a combination of microstrip line as RH part and lumped components as LH part, considered as the intermediate part of multi-stage GVD. In general, the component values associated with them are computed by the methodology followed in [48]. A LC type of matching circuit is introduced to avoid the tedious calculations in reducing the complexity [39].

Considering implementation, a large-signal S-parameter circuit simulation environment is setup in the ADS solver to determine the various outcomes associated with the RF-EH application. Here, the η_0 is calculated by considering equation (6), where the CRLH and LC-based multi-stage rectifier circuit/s reported for the first time in the literature are analyzed for the input power

Table 4. Performance characteristics of SYPMA-MTS integrated with the proposed rectifier circuits (I, II) over existing ones in [39, 40, 48–54]

Ref.	Antenna gain	P_{in}	η_0	V_{out}
39.	6.82 dBic (CP)	5 dBm	19%	1.5 V
40.	4.92 dBic (CP)	5 dBm	25%	—
48.	5.85 dBic (CP)	5 dBm	50%	—
49.	7.8 dBi (LP)	5 dBm	5%	0.5 V
50.	6.9 dBi (LP)	5 dBm	—	0.1 V
51.	7.3 dBi (LP)	5 dBm	14%	1.1 V
52.	5.01 dBic (CP)	5 dBm	43%	1.16 V
53.	5.5 dBi (LP)	5 dBm	5%	0.2 V
54.	2.6 dBi (LP)	5 dBm	55%	—
P2.	8.45 dBic (CP)	5 dBm	43% (I)	1.7 V (I)
	8.45 dBic (CP)	5 dBm	61% (II)	2.1 V (II)

https://doi.org/10.1017/S1759078722000988 Published online by Cambridge University Press

levels (P_{in}) from − 10 to + 20 dBm respectively, which covers the possibility of low-input power levels at 5 GHz.

$$\eta_0(\%) = \frac{P_{load}}{P_{incident}} = \frac{V_{out}^2}{P_{in} \times R_{load}} \quad (6)$$

On the final note, at P_{in} = 5 dBm, V_{out} is 1.7 V, with η_0 as 43% for CRLH-based GVD circuit (I), whereas, V_{out} is 2.1 V, with η_0 as 61% for LC-based GVD circuit (II). Here, the maximum attainable V_{out} is 5.39 V (for I) and 5.4 V (for II), along with the maximum attainable η_0 as 56.28% (for I) and 73.82% (for II) are presented in Figs 6(b) and (c). By looking into the prospective of earlier RF-EH system designs [39, 40, 48–54], the proposed antenna + rectifier design reported here, especially LC-based GVD circuit (II), depicts higher outcomes over the existing literatures, as shown in Table 4.

Conclusion

This research paper highlights about a high-gain and broadband circularly polarized printed monopole antenna loaded with the MTS reflector. It achieves effectiveness due to its simple configuration and operates with the features of 45.48% IBW and 25.25% ARBW responses. By loading the MTS reflector, CP performances, antenna gain, and the radiation parameters are improved. The peak antenna gain lies between 7.5 and 8.5 dBi with directional characteristics, and improved FBR of − 21.5 dBic. The antenna efficiency of > 75% in their designated bands is also observed. To test its potential utility toward the RF-EH application, CRLH and LC-based GVDs are integrated with the antenna system. The LC-based GVD circuit (II) is more effective than CRLH-based GVD circuit (I) with V_{out} of 2.1 V, η_0 as 61%, and V_{out} of 1.7 V, η_0 as 43%, which proposes effective solution toward implementing rectifiers than those reported in [39, 40, 48–54].

References

1. **AT Abed** (2020) A novel coplanar antenna butterfly structure for portable communication devices. *IEEE Antennas and Propagation Magazine* **62**, 83–89.
2. **BY Toh, R Cahill and VF Fusco** (2003) Understanding and measuring circular polarization. *IEEE Transactions on Education* **46**, 313–318.
3. **MJ Maybell** (2019) A polarization basics diagram [historical corner]. *IEEE Antennas and Propagation Magazine* **61**, 130–135.
4. **J Wu and K Sarabandi** (2017) Compact omnidirectional circularly polarized antenna. *IEEE Transactions on Antennas and Propagation* **65**, 1550–1557.
5. **S Mathew, M Ameen, MP Jayakrishnan, P Mohanan and K Vasudevan** (2016) Compact dual polarised V slit, stub and slot embedded circular patch antenna for UMTS/WiMAX/WLAN applications. *Electronics Letters* **52**, 1425–1426.
6. **S Shekhawat, P Sekra, D Bhatnagar, VK Saxena and JS Saini** (2010) Stacked arrangement of rectangular microstrip patches for circularly polarized broadband performance. *IEEE Antennas and Wireless Propagation Letters*, **9**, 910–913.
7. **A Gupta and RK Chaudhary** (2018) The metamaterial antenna: a novel miniaturized dual-band coplanar waveguide-fed antenna with backed ground plane. *IEEE Antennas and Propagation Magazine*, **60**, 41–48.
8. **FA Asadallah, J Costantine and Y Tawk** (2018) A multiband compact reconfigurable PIFA based on nested slots. *IEEE Antennas and Wireless Propagation Letters* **17**, 331–334.
9. **H Wong, KK So, KB Ng, KM Luk, CH Chan and Q Xue** (2010) Virtually shorted patch antenna for circular polarization. *IEEE Antennas and Wireless Propagation Letters* **9**, 1213–1216.
10. **D Elsheakh and E Abdallah** (2017) Ultra-wide-bandwidth (UWB) microstrip monopole antenna using split ring resonator (SRR) structure. *International Journal of Microwave and Wireless Technologies* **10**, 123–132.
11. **ST Ko, BC Park and JH Lee** (2013) Dual band circularly polarized patch antenna with first positive and negative modes. *IEEE Antennas and Wireless Propagation Letters* **12**, 1165–1168.
12. **H Kuhestani, M Rahimi, Z Mansouri, FB Zarrabi and R Ahmadian** (2015) Design of a compact patch antenna based on metamaterial for WiMAX applications with circular polarization. *Microwave and Optical Technology Letters* **57**, 357–360.
13. **T Cai, GM Wang, XF Zhang and J-P Shi** (2015) Low-profile compact circularly-polarized antenna based on fractal metasurface and fractal resonator. *IEEE Antennas and Wireless Propagation Letters*, **14**, 1072–1076.
14. **W Cao, X Lv, Z Zeng, J Jin and H Liu** (2019) Bandwidth enhanced dual-band patch-coupling microstrip antenna with omnidirectional CP and unidirectional CP characteristics. *IET Microwaves, Antennas & Propagation* **13**, 584–590.
15. **N Nasimuddin, ZN Chen and X Qing** (2012) A compact circularly polarized cross-shaped slotted microstrip antenna. *IEEE Transactions on Antennas and Propagation* **60**, 1584–1588.
16. **J Lin and Q Chu** (2018) Enhancing bandwidth of CP microstrip antenna by using parasitic patches in annular sector shapes to control electric field components. *IEEE Antennas and Wireless Propagation Letters* **17**, 924–927.
17. **KY Lam, K-M Luk, KF Lee, H Wong and KB Ng** (2011) Small circularly polarized U-slot wideband patch antenna. *IEEE Antennas and Wireless Propagation Letters* **10**, 87–90.
18. **R Kumar and RK Chaudhary** (2018) Circularly polarized rectangular DRA coupled through orthogonal slot excited with microstrip circular ring feeding structure for Wi–MAX applications. *International Journal of RF and Microwave Computer-Aided Engineering* **28**, e21153.
19. **K Wang and H Wong** (2015) A circularly polarized antenna by using rotated-stair dielectric resonator. *IEEE Antennas and Wireless Propagation Letters* **14**, 787–790.
20. **S Ghosh and A Chakrabarty** (2016) Dual band circularly polarized monopole antenna design for RF energy harvesting. *IETE Journal of Research* **62**, 9–16.
21. **A Altaf, Y Yang, K-Y Lee and KC Hwang** (2015) Circularly polarized spidron fractal dielectric resonator antenna. *IEEE Antennas and Wireless Propagation Letters* **14**, 1806–1809.
22. **R Kumar, SR Thummaluru and RK Chaudhary** (2019) Improvements in Wi-MAX reception: a new dual-mode wideband circularly polarized dielectric resonator antenna. *IEEE Antennas and Propagation Magazine* **61**, 41–49.
23. **Z-L Zhang, K Wei, J Xie, J-Y Li and L Wang** (2019) The new C-shaped parasitic strip for the single-feed circularly polarized (CP) microstrip antenna design. *International Journal of Antennas and Propagation* **2019**, 5427595.
24. **T Yue, ZH Jiang and DH Werner** (2016) Compact, wideband antennas enabled by interdigitated capacitor-loaded metasurfaces. *IEEE Transactions on Antennas and Propagation* **64**, 1595–1606.
25. **N Hussain, SI Naqvi, WA Awan and TT Le** (2020) A metasurface-based wideband bidirectional same sense circularly polarized antenna. *International Journal of RF and Microwave Computer-Aided Engineering* **30**, e22262.
26. **Z Wu, L Li, Y Li and X Chen** (2016) Metasurface superstrate antenna with wideband circular polarization for satellite communication application. *IEEE Antennas and Wireless Propagation Letters* **15**, 374–377.
27. **Q Chen, H Zhang, L-C Yang, X-F Zhang and Y-C Zeng** (2018) Wideband and low axial ratio circularly polarized antenna using AMC-based structure polarization rotation reflective surface. *International Journal of Microwave and Wireless Technologies* **10**, 1058–1064.
28. **W Wang, K-W Tam, W-W Choi, W Che and HT Hui** (2014) Novel polarization rotation technique based on an artificial magnetic conductor and its application in a low-profile circular polarization antenna. *IEEE Transactions on Antennas and Propagation* **62**, 6206–6216.
29. **PK Rajanna, K Rudramuni and K Kandasamy** (2020) Characteristic mode-based compact circularly polarized metasurface antenna for in-band

https://doi.org/10.1017/S1759078722000988 Published online by Cambridge University Press

RCS reduction. *International Journal of Microwave and Wireless Technologies* **12**, 131–137.
30. **M Ameen and RK Chaudhary** (2021) Metamaterial circularly polarized antennas: integrating an epsilon negative transmission line and single split ring-type resonator. *IEEE Antennas and Propagation Magazine* **63**, 60–77.
31. **W Lin and H Wong** (2017) Wideband circular-polarization reconfigurable antenna with L-shaped feeding probes. *IEEE Antennas and Wireless Propagation Letters* **16**, 2114–2117.
32. **W Wang, W Che, H Jin, W Feng and Q Xue** (2015) A polarization-reconfigurable dipole antenna using polarization rotation AMC structure. *IEEE Transactions on Antennas and Propagation* **63**, 5305–5315.
33. **W Lin, S-L Chen, RW Ziolkowski and YJ Guo** (2018) Reconfigurable, wideband, low-profile, circularly polarized antenna and array enabled by an artificial magnetic conductor ground. *IEEE Transactions on Antennas and Propagation* **66**, 1564–1569.
34. **L Huang, H Yu-Xuan, L Zhan-Wei, C Shu-Ting, X Xiao-Ming and G Jing** (2020) Design of a compact wideband CP metasurface antenna. *International Journal of RF and Microwave Computer-Aided Engineering* **30**, e22332.
35. **A Dastranj** (2017) Very small planar broadband monopole antenna with hybrid trapezoidal-elliptical radiator. *IET Microwaves, Antennas & Propagation* **11**, 542–547.
36. **M Mathur, A Agrawal, G Singh and SK Bhatnagar** (2018) A compact coplanar waveguide fed wideband monopole antenna for RF energy harvesting applications. *Progress in Electromagnetics Research M* **63**, 175–184.
37. **R Pandey, AK Shankhwar and A Singh** (2020) Design, analysis, and optimization of dual side printed multiband antenna for RF energy harvesting applications. *Progress in Electromagnetics Research C* **102**, 79–91.
38. **BR Behera, PR Meher and SK Mishra** (2020) Microwave antennas – an intrinsic part of RF energy harvesting systems: a contingent study about its design methodologies and state-of-art technologies in current scenario. *International Journal of RF and Microwave Computer-Aided Engineering* **30**, e22148.
39. **BR Behera, PR Meher and SK Mishra** (2021) Metasurface superstrate inspired printed monopole antenna for RF energy harvesting application. *Progress in Electromagnetics Research C* **110**, 119–133.
40. **BR Behera, P Srikanth, PR Meher and SK Mishra** (2020) A compact broadband circularly polarized printed monopole antenna using twin parasitic conducting strips and rectangular metasurface for RF energy harvesting application. *AEU-International Journal of Electronics and Communication* **120**, 153233.
41. **A Mohanty, BR Behera and N Nasimuddin** (2021) Hybrid metasurface loaded tri-port compact antenna with gain enhancement and pattern diversity. *International Journal of RF and Microwave Computer-Aided Engineering* **31**, e22795.
42. **D Surender, T Khan, FA Talukdar, A De, Yahia MM Antar and AlP Freundorfer** (2020) Key components of rectenna system: a comprehensive survey. *IETE Journal of Research (Latest Articles)* 1–27.
43. **D Surender, T Khan, FA Talukdar and Yahia MM Antar** (2021) Rectenna design and development strategies for wireless applications: a review. IEEE Antennas and Propagation Magazine, 2–15 (early access).
44. **D Surender, Md Halimi, T Khan, FA Talukdar, SK Koul and Yahia MM Antar** (2022) 2.45 GHz Wi-Fi band operated circularly polarized rectenna for RF energy harvesting in smart city applications. *Journal of Electromagnetic Waves and Applications* **36**, 407–423.
45. **D Surender, Md Halimi, T Khan, FA Talukdar, AA Kishk, Yahia MM Antar and SR Rengarajan** (2022) Semi-annular-ring slots loading for broadband circularly polarized DR-rectenna for RF energy harvesting in smart city environment. *AEU-International Journal of Electronics and Communications* **147**, 154143.
46. **D Surender, Md Halimi, T Khan, FA Talukdar and Yahia MM Antar** (2022) A 90° twisted quarter-sectored compact and circularly polarized DR-rectenna for RF energy harvesting applications. *IEEE Antennas and Wireless Propagation Letters* **21**, 1139–1143.
47. **D Surender, Md Halimi, T Khan, FA Talukdar and Yahia MM Antar** (2022) A triple band rectenna for RF energy harvesting in smart city applications. *International Journal of Electronics* 1–15.
48. **AM Jie, N Nasimuddin, MF Karim and KT Chandrasekaran** (2019) A wide-angle circularly polarized tapered-slit patch antenna with a compact rectifier for energy-harvesting systems. *IEEE Antennas and Propagation Magazine* **61**, 94–111.
49. **FS Mohd Noor, Z Zakaria, H Lago and MAM Said** (2019) Dual-band aperture-coupled rectenna for radio frequency energy harvesting. *International Journal of RF and Microwave Computer-Aided Engineering* **29**, e21651.
50. **A Bakkali, J Pelegri-Sebastia, T Sogorb, V Llario and A Bou-Escriva** (2016) A dual-band antenna for RF energy harvesting systems in wireless sensor networks. *Journal of Sensors* **2016**, 5725836.
51. **N Singh, BK Kanaujia, MT Beg, Mainuddin, T Khan and S Kumar** (2018) A dual polarized multiband rectenna for RF energy harvesting. *AEU-International Journal of Electronics and Communication* **93**, 123–131.
52. **D Surender, Md Halimi, T Khan, FA Talukdar and Yahia MM Antar** (2021) Circularly polarized DR-rectenna for 5G and Wi-Fi bands RF energy harvesting in smart city applications. *IETE Technical Review* 1–15.
53. **OM Dardeer, HA Elsadek, EA Abdallah and HM Elhennawy** (2019) A dual band circularly polarized rectenna for RF energy harvesting applications. *ACES Journal* **34**, 1594–1600.
54. **KT Chandrasekaran, K Agarwal, N Nasimuddin, A Alphones, R Mittra and MF Karim** (2020) Compact dual-band metamaterial-based high-efficiency rectenna: an application for ambient electromagnetic energy harvesting. *IEEE Antennas and Propagation Magazine* **62**, 18–29.

Bikash Ranjan Behera has received the M.E. degree with specialization in Wireless Communication, Department of Electronics and Communication Engineering from Birla Institute of Technology Mesra, Ranchi, Jharkhand, India in 2016. He is currently pursuing Ph.D. in RF and Microwaves, Department of Electronics and Telecommunication Engineering with the International Institute of Information Technology Bhubaneswar, Odisha, India. His research interests are RF energy harvesting systems and metamaterials-inspired antenna designing.

Sanjeev Kumar Mishra (SM'16) has received Ph.D. from the Department of Electrical Engineering from the Indian Institute of Technology Bombay, Mumbai, India in 2012. At present, he is working as an Assistant Professor in the Department of Electronics and Telecommunication Engineering with the International Institute of Information Technology Bhubaneswar, Odisha, India. He has authored and co-authored in more than 70 papers in reputed journals and conferences. He has two patents and written book on planar antennas. Dr. Mishra is the recipient of Young Scientist Award (YSA) at AP-RASC'13, Taiwan. His research interests are RF and microwave circuits and system design,microwave remote sensing and sensors, and measurements. He is the senior member of IEEE and reviewer of *IEEE Antennas and Wireless Propagation Letters*, *IET Microwaves, Antenna & Propagation*, *Progress in Electromagnetic Research*, etc., and a reviewer for research projects in Science and Engineering Research Board for Department of Science and Technology (DST- SERB), Government of India.

https://doi.org/10.1017/S1759078722000988 Published online by Cambridge University Press